

# Kinetic-Anisotropy-Induced Ordering-Orientation Transition in Epitaxial Growth: A Method to Synthesize Ordering-Orientation Superlattices

Lin Shi and Jun Ni

*Department of Physics and Key Laboratory of Atomic and Molecular Nanoscience (Ministry of Education),  
Tsinghua University, Beijing 100084, People's Republic of China*

(Received 24 March 2006; published 21 September 2006)

The epitaxial growth has a distinct kinetic feature that the lateral surface diffusion is faster than the longitudinal bulk diffusion. We show there is an ordering-orientation transition of alloy films with the change of growth rate due to this kinetic anisotropy. As an example, we have calculated the epitaxial growth of CoPt alloy films on the Pt buffer layer. We show the ordered structure of CoPt films changes from the  $L1_0$  [001] (a compositional modulation along the [001] direction) variant to the  $L1_0$  [100] variant with the increase of growth rate. This ordering-orientation transition also occurs with the decrease of temperature at adequate growth rate. Based on this mechanism, we propose a simple method to synthesize the ordering-orientation superlattices.

DOI: [10.1103/PhysRevLett.97.126105](https://doi.org/10.1103/PhysRevLett.97.126105)

PACS numbers: 81.15.Aa, 64.60.Cn, 68.65.Cd

The epitaxial methods have been extensively used in alloy growth for the purpose of fabricating superlattices and various ordered structures [1–8]. The ordered structures of alloys and other low dimensional structures have distinct properties for applications. The epitaxial growth is a nonequilibrium growth process. The kinetic feature of growth is one of the controlling factors in the formation of alloy structures. It is found that the kinetics of growth layer is affected by the underlayer structure, which causes the occurrence of a kinetically induced oscillatory ordered structure [9]. The relaxation competition between ordering and phase separation leads to novel ordering [10]. The formations of various self-organized structures of alloys are attributed to the kinetic processes in the epitaxial growth [1,11].

In the epitaxial growth, there is a distinct kinetic feature that the lateral surface atomic diffusion is faster than the longitudinal bulk diffusion, which we call the kinetic anisotropy. In this Letter, we show there is an ordering-orientation transition of alloy films with the increase of growth rate due to the kinetic anisotropy. Let us consider the growth of fcc alloy films with the  $L1_0$  bulk structure, which has three equivalent orientation variants: the  $L1_0$  [100], [010], and [001] ordered structures as shown in Fig. 1. For an alloy film, the [001] orientation variant is not equivalent to the [100] and [010] orientation variants due to the symmetry loss along the  $z$  axis of growth direction by interaction with the substrate. In the low growth rate, the kinetic process is governed by the bulk diffusion and the grown structure will be the ground state. When the energy of the longitudinal  $L1_0$  [001] variant is lower than that of the lateral  $L1_0$  [100] and [010] variants, the grown structure will be the  $L1_0$  [001] variant. In the high growth rate, the kinetic process is governed by the fast lateral surface atomic diffusion. The grown structure will be the  $L1_0$  [100] and [010] variants. Thus there is a kinetic-anisotropy-induced ordering-orientation transition when

the growth rate is changed. We show this mechanism can be used to synthesize the ordering-orientation superlattices. If the species are magnetocrystalline anisotropy, we can synthesize the anisotropic magnetic superlattice which has modulated magnon energy gap existing in the energy band of spin wave excitation and adjusted magnon spectrum.

We consider CoPt alloy as an example. The CoPt alloy films show excellent magnetic properties with high magnetic anisotropy, coercivity, and large Kerr rotation, which attracted considerable interest both for scientific researches and for the applications of high density magnetic record [12–14]. The disordered CoPt alloy has an fcc structure and the ordered phase is the  $L1_0$  structure. The magnetic anisotropy and Kerr rotation of CoPt alloys are very sensitive to the chemical ordering [12,13]. The epitaxial methods are used to prepare the ordered CoPt alloy films [12–14]. When the buffer layer is Pt layer and the substrate is MgO(001), the CoPt alloy films grown by the epitaxial methods form the  $L1_0$  ordered structure along the [001] direction [13].

We consider an fcc film of CoPt alloy grown in the [001] direction. During the epitaxial growth process, the system consists of three components, two atomic species (Co and Pt) and vacancy ( $V$ ). The lattice of (001) planes of an fcc alloy is the square lattice. To describe the ordering of the

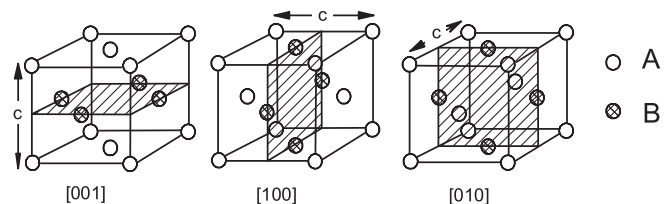


FIG. 1. The [001], [100], and [010] variants of the  $L1_0$  ordered structure.

system, we divide the square lattice of each layer into two sublattices ( $\alpha$  and  $\beta$ ). The configurations of the system are described by the site probabilities in the kinetic mean-field approximation of growth [9,15].  $P_i^s(m, t)$  is the probability occupied by  $i$  ( $=$  Co, Pt, V) species in  $s$  ( $=$   $\alpha$ ,  $\beta$ ) sublattices on the  $m$ th growth layer at time  $t$ . The concentrations of each layer are related to the site probability  $P_i^s$  as follows:  $x_i(m) = [P_i^\alpha(m) + P_i^\beta(m)]/2$ . The phase structures are described by the following order parameters in each layer related to the site probability  $P_i^s$ . The order parameter in the [100] direction is  $\eta_{[100]}(m) = P_{\text{Co}}^\alpha(m) - P_{\text{Co}}^\beta(m)$ . The order parameter in the [001] direction [13] is:  $\eta_{[001]}(m) = |x_{\text{Co}}(m) - x_{\text{Pt}}(m)|$ . The order parameters equal to 1 corresponds the complete ordering. When the order parameter of an orientation variant is zero, the system is disordered for this orientation variant. When the order parameter takes fractional value, the ordering in that direction is partial, which means the corresponding sublattices are not completely occupied by one species of atoms (Co or Pt atoms).

The kinetics of growth is described by the following differential equations with all the three contributions from the diffusion, evaporation, and adsorption processes [9,15]:

$$\frac{dP_i^s(m)}{dt} = \sum_j \sum_{s'} (Y_{ji}^{ss'} - Y_{ij}^{ss'}) + Z_i^s(m) + X_i^s(m) \quad (1)$$

where the first sum runs over all nearest sites of the  $i$  species on the site  $s$ .  $Y_{ij}^{ss'}$  represents the exchange probability between species  $i$  on the site  $s$  and species  $j$  on the site  $s'$  per unit time.  $X_i^s(m)$  is the adsorption probability of the species  $i$  on the sublattice  $s$  on the  $m$ th layer per unit time.  $Z_i^s(m)$  is the evaporation probability of the species  $i$  from the  $s$  sublattice on the  $m$ th layer per unit time.  $Y_{ij}^{ss'}$  is proportional to the atomic exchange rate, the site probabilities  $P_i^s$  and  $P_j^{s'}$ , the vacancy probabilities of the over sites and a factor describing the effect of the neighboring sites for the atom-vacancy exchange [16,17].  $X_i^s(m)$  is proportional to the adsorption rate and the vacancy probability  $P_V^s(m)$ . An atom can only evaporate when the sites over it are occupied by vacancies.  $Z_i^s(m)$  is proportional to the evaporation rate, the site probability  $P_i^s(m)$  of the evaporation atom, the chemical potential factor  $\exp(-\mu_i/k_B T)$  ( $\mu_i$  is the chemical potential of the  $i$  species), and the bond broken factor  $V_i^s$  for evaporation. The adsorption rate is related to the evaporation rate by the detailed balance condition [15]. To grow the equiatomic CoPt alloy, we take the chemical potentials  $\mu_{\text{Co}} = \mu_{\text{Pt}}$ . The differential equations are solved numerically by the Runge-Kutta method. Initially the growth layer is empty and the buffer layer is Pt layer.

In the kinetic process, we take the activation energy of atomic diffusion as follows: The activation energy for the surface diffusion of Pt atoms is taken as 0.47 eV which is the activation energy for Pt diffusion on the Pt(001) surface [18] and the activation energy for the surface diffusion of Co atoms is taken as 0.58 eV which is the activation energy

for Co diffusion on the Co(001) surface [19]. For the bulk diffusion in CoPt(001) multilayers, the activation energy is 1.1 eV [20]. Since the atomic jumping frequency is approximately  $10^{14} \text{ s}^{-1}$ , we take the prefactor  $\nu_D = \tau_D^{-1} = 10^{14} \text{ s}^{-1}$ . The surface diffusion is much faster than the bulk diffusion for the CoPt epitaxial growth.

In order to calculate the ordering process, we have determined the interaction energy parameters in the kinetic equations by performing the calculations of total energies of structures using VASP (the Vienna *ab initio* simulation package) [21]. The approach is based on an iterative solution of the Kohn-Sham equations of the density-functional theory in a plane-wave basis set with the Vanderbilt ultrasoft pseudopotentials [22]. The exchange correlation functional with the generalized gradient approximation is given by Perdew *et al* [23]. We set the plane-wave cutoff energy to be 500 eV. The tolerance of the energy convergence is  $10^{-4}$  eV. The energies of Co, Pt,  $\text{Co}_3\text{Pt}(L1_2)$ ,  $\text{CoPt}(L1_1)$ ,  $\text{CoPt}(L1_0)$ , and  $\text{CoPt}_3(L1_2)$  structures are calculated. The interaction parameters are determined by the total energies. In order to determine the accurate interaction parameters, we have employed the same size of supercells for different structures. The calculations are performed on the  $(2 \times 2 \times 1)$  supercells containing 16 atoms. A mesh of gamma centered grids  $5 \times 5 \times 9$  is used to sample the Brillouin zone. We consider the nearest and next nearest-neighbor interaction energies. Based on the calculated total energies, we deduce the interaction energies as shown in Table I. The interaction energies affect the ordering only through the interchange energies  $J^{(k)} = \frac{1}{4}(E_{\text{CoCo}}^{(k)} + E_{\text{PtPt}}^{(k)} - 2E_{\text{CoPt}}^{(k)})$ .  $E_{ij}^{(k)}$  are the  $k$ th nearest-neighbor interaction energies between  $i$  and  $j$  atomic species. Since the interaction energies for the next nearest-neighbors are small, we do not consider the effect of the next nearest-neighbor interaction energies on the atomic jumping rate. For the fcc lattice, the order-disorder transition temperature is about  $T_C = 1.8J^{(1)}/k_B$  by the cluster variation method [24], where  $J^{(1)}$  is the interchange energy in eV and  $k_B = 8.620 \times 10^{-5} \text{ eV K}^{-1}$  is the Boltzmann constant. Based on the interchange energy, the order-disorder transition temperature of CoPt alloy is about  $T_C = 1070 \text{ K}$ , which is in agreement with the result of  $T_C = 1110 \text{ K}$  in Ref. [25]. For the ordered structures of CoPt films grown on the Pt buffer layer, our calculations show that the energy of the  $L1_0$  [001] ordered structure is lower than that of the  $L1_0$  [100] ordered structure, which agrees with the experimental results [13].

With these energy parameters, we have calculated the epitaxial growth process of CoPt alloy films in the [001]

TABLE I. The energy parameters for the ordering of CoPt alloys (eV).

$E_{\text{CoPt}}^{(1)}$	$E_{\text{CoCo}}^{(1)}$	$E_{\text{PtPt}}^{(1)}$	$J^{(1)}$	$J^{(2)}$
-1.084	-1.053	-0.910	0.0512	-0.001

direction on the Pt buffer. We define the ratio  $\kappa = \omega/\nu_D$  between the deposition rate  $\omega$  and atomic jumping frequency  $\nu_D$  and use  $\kappa$  as a parameter. We find the average order parameter in the [001] direction increases with the increase of growth temperature, which is in agreement with the experimental results [13].

In order to show how the variants of the  $L1_0$  ordered structure change with the growth parameters, we have calculated the variation of the order parameters with  $\kappa$  and the growth temperature. In the experiment by Ersen *et al.*, [13] the CoPt film is highly ordered at growth temperature of 800 K and disordered at about 300 K. We choose the moderate growth temperature of  $T = 570$  K to calculate the variation of the order parameters with the change of  $\kappa$  as shown in Fig. 2(a). It can be seen that the average order parameter  $\overline{\eta}_{[001]}$  decreases with the increase of  $\kappa$ . The average order parameter  $\overline{\eta}_{[100]}$  has a peak at  $\kappa = 3.75 \times 10^{-6}$ . The difference between the surface and bulk diffusion contributes to this kinetic phenomenon. When  $\kappa$  is small, the atoms have enough diffusion time to form the stable  $L1_0$  [001] ordered structure and the grown structure is the  $L1_0$  [001] ordered structure. When  $\kappa$  is increased, the evolution time is shortened to restrain the bulk diffusion. In this case, the surface diffusion governs the ordering process due to the fast surface diffusion. The ordering in the growth layer results in the  $L1_0$  [100] ordered structure. When  $\kappa$  continues to increase, the evolution time is very short, both the bulk and surface diffusion are restrained, and the ordered structure are not formed. As shown in Fig. 2(a), with the increase of  $\kappa$ , the ordering orientation of the grown structure first changes from the [001] direction to the [100] direction and then the grown structure changes to the disordered one. For comparison, we have also calculated the variation of the order parameters with the increase of  $\kappa$  using the Monte Carlo method [26] with the same growth mechanism and energy parameters as those used in the mean-field approach. The simulations are carried out on square  $32 \times 32$  lattices with eight growing layers. The periodic boundary condition in  $x$ - $y$  plane is used. Twenty repeated growth procedures are used for the average. The sublattice average occupations are used to

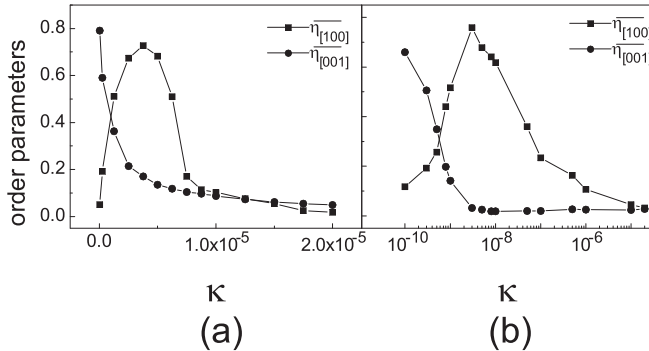


FIG. 2. The average order parameters of 8 layer films as a function of  $\kappa$  with  $T = 570$  K, (a) results of the mean-field approach and (b) results of the Monte Carlo method.

calculate the order parameters. As shown in Fig. 2(b), the curves of the order parameters are consistent with those calculated by the mean-field approach. The Monte Carlo method gives a slower ordering kinetics [correspondingly smaller peak value of  $\kappa$  in Fig. 2(b)] than the mean-field approach, which is in agreement with the results of Ref. [27] showing that the evolution time in the pair approximation for the long range order to reach the equilibrium value is longer than that in the point approximation. Figure 3 shows the temperature dependence of the ordering-orientation transition. We choose four different  $\kappa$  to calculate the variation of the order parameter with the growth temperature. As shown in Fig. 3,  $\overline{\eta}_{[001]}$  increases with the increase of the growth temperature and  $\overline{\eta}_{[100]}$  has a temperature peak. The peak value of  $\overline{\eta}_{[100]}$  decreases with the increase of  $\kappa$ , but the corresponding peak temperature increases with the increase of  $\kappa$ . The small shoulder plateau neighboring the peak in the curve of  $\overline{\eta}_{[100]}$  is found to be due to the appearance of the oscillatory ordered structures [9].

Based on the mechanism of the ordering-orientation transition, we can grow the two different ordering-orientation structures by changing the growth rate. If we periodically change the growth rate to grow the film, the two different ordering-orientation structures form alternatively, which leads to an ordering-orientation superlattice. The superlattice with the ordering reorientated per 12 layers is shown in Fig. 4(a). We choose the growth temperature  $T = 570$  K. We change the growth rate per 12 layers from  $\kappa = 2.5 \times 10^{-7}$  to  $3.75 \times 10^{-6}$  and grow 48 layers. The order parameters of 48 layers are shown in Fig. 4(b). The system first forms the  $L1_0$  [001] ordered structure in layers 1–12 with  $\kappa = 2.5 \times 10^{-7}$ , then forms the  $L1_0$  [100] ordered structure in layers 13–24 with  $\kappa =$

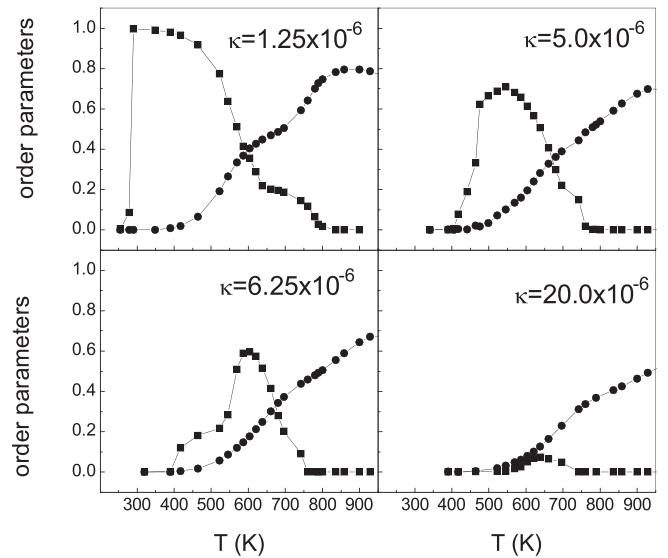


FIG. 3. The average order parameters of 8 layer films as a function of temperature, where circles represent  $\overline{\eta}_{[001]}$  and squares represent  $\overline{\eta}_{[100]}$ .

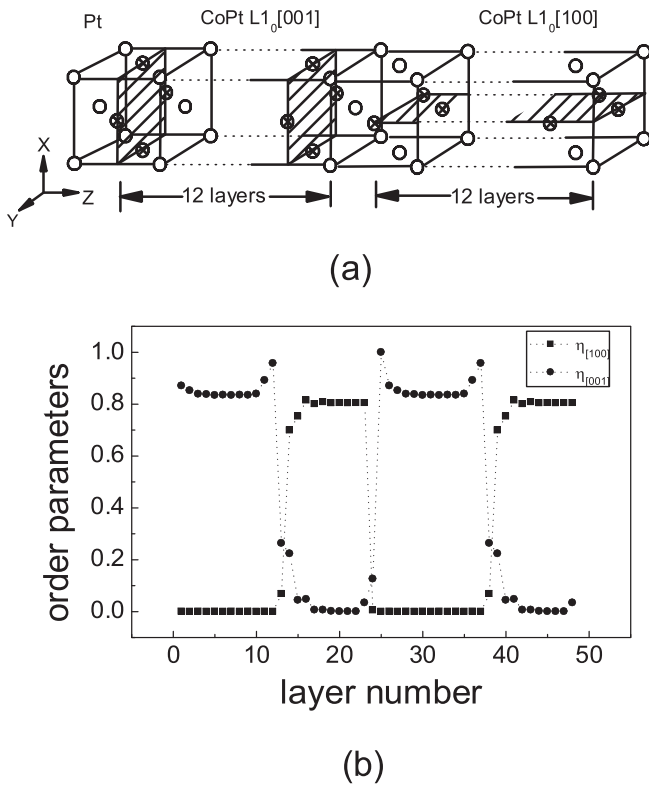


FIG. 4. (a) The superlattice with the ordering-orientation transition per 12 layers. (b) The order parameters of the ordering-orientation superlattice.

$3.75 \times 10^{-6}$ . Then we change the chemical potential to grow one Pt rich layer for the 25th layer in order to make the transition abrupt. We grow layers 26–48 at the same condition as layers 1–24 and get the same structure. In this way, the ordering orientation periodically changes as shown in Fig. 4(b). The supercell of the superlattice can be changed by adjusting the variation periodicity of  $\kappa$ .

The magnetic anisotropy and Kerr rotation of CoPt alloy are sensitive to the structure and the order parameters of the structure. The ordered variant boundaries can form pinning sites that impede the movement of magnetic domain walls and leads to high coercivity [14]. The orientation variant transition from the  $L1_0$  [001] ordered structure to the  $L1_0$  [100] ordered structure with the change of growth rate can be used to regulate the formation of the variant boundaries.

In conclusion, we have investigated the effect of the kinetic anisotropy on the formation of structures in the epitaxial growth of alloy films. In the CoPt epitaxial growth, we show that the ordering orientation of the  $L1_0$  ordered structure changes from the [001] direction to the [100] direction with the increase of the growth rate. We have also calculated the temperature dependence of the ordering-orientation transition. With the increase of temperature, the average order parameter  $\overline{\eta_{[001]}}$  increase and the average order parameter  $\overline{\eta_{[100]}}$  has a temperature peak.

Based on the mechanism of the ordering-orientation transition induced by the kinetic anisotropy, we propose a simple method to synthesize the ordering-orientation superlattice by periodically changing the growth rate. This mechanism can also be used to form other nanostructures with two different ordered structures, one formed by the lateral surface diffusion and the other formed by the longitudinal bulk diffusion, when the surface structure is different with the truncated bulk structures during the epitaxial growth.

This research was supported by the National Natural Science Foundation of China (Grants No. 10474049 and No. 10274036) and the National Basic Research Program of China.

- 
- [1] P. Venezuela *et al.*, Nature (London) **397**, 678 (1999).
  - [2] Y.L. Foo *et al.*, Phys. Rev. Lett. **90**, 235502 (2003).
  - [3] C.A. Wang, C.J. Vineis, and D.R. Calawa, Appl. Phys. Lett. **85**, 594 (2004).
  - [4] H.N. Lee *et al.*, Nature (London) **433**, 395 (2005).
  - [5] J.H. He *et al.*, Phys. Rev. Lett. **96**, 056105 (2006).
  - [6] *Spontaneous Ordering in Semiconductor Alloys*, edited by A. Mascarenhas (Kluwer Academic, New York, 2002).
  - [7] J.H. Li *et al.*, Phys. Rev. Lett. **91**, 106103 (2003).
  - [8] E.D. Tober *et al.*, Phys. Rev. Lett. **81**, 1897 (1998).
  - [9] L. Shi and J. Ni, Phys. Rev. B **69**, 155428 (2004).
  - [10] H. Reichert *et al.*, Phys. Rev. Lett. **95**, 235703 (2005).
  - [11] I. Daruka and J. Tersoff, Phys. Rev. Lett. **95**, 076102 (2005).
  - [12] B.M. Lairson and B.M. Clemens, Appl. Phys. Lett. **63**, 1438 (1993).
  - [13] O. Ersen *et al.*, J. Appl. Phys. **93**, 2987 (2003).
  - [14] R. A. Ristau *et al.*, J. Appl. Phys. **86**, 4527 (1999).
  - [15] Y. Saito and H. Müller-Krumbhaar, J. Chem. Phys. **70**, 1078 (1979).
  - [16] H. T. Shi and J. Ni, Phys. Rev. B **65**, 115422 (2002).
  - [17] L. Q. Chen and J. A. Simmons, Acta Metall. Mater. **42**, 2943 (1994).
  - [18] G.L. Kellogg and P.J. Feibelman, Phys. Rev. Lett. **64**, 3143 (1990).
  - [19] R. A. Miron and K. A. Fichthorn, Phys. Rev. B **72**, 035415 (2005).
  - [20] P. C. McIntyre, D. T. Wu, and M. Nastasi, J. Appl. Phys. **81**, 637 (1997).
  - [21] G. Kresse and J. Hafner, Phys. Rev. B **47**, R558 (1993); **49**, 14 251 (1994); G. Kresse and J. Furthmüller, Phys. Rev. B **54**, 11 169 (1996).
  - [22] D. Vanderbilt, Phys. Rev. B **41**, R7892 (1990).
  - [23] J. P. Perdew *et al.*, Phys. Rev. B **46**, 6671 (1992).
  - [24] A. Finel and F. Ducastelle, Europhys. Lett. **1**, 135 (1986).
  - [25] J.M. Sanchez *et al.*, J. Phys. Condens. Matter **1**, 491 (1989).
  - [26] D.P. Landau and K. Binder, *A Guide to Monte Carlo Simulations in Statistical Physics* (Cambridge University Press, Cambridge, 2000).
  - [27] L. Q. Chen, Phys. Rev. B **58**, 5266 (1998).